19th AIAA Aerodynamic Decelerator Systems Technology Conference and Seminar
21 - 24 May 2007, Williamsburg, VA

R07-30

AIAA 2007-2514

Autonomous Large Parafoil Guidance, Navigation, and Control System Design Status

David W. Carter[1], Sean George[2], Philip D. Hattis[3], Marc W. McConley[4], Scott A. Rasmussen[5], Leena Singh[6]
Draper Laboratory, Cambridge, MA, 02459

and

Steve Tavan[7]
Natick Soldier Research, Development and Engineering Center, Natick, MA 01760

Demonstration of autonomous Guidance, Navigation, and Control (GN&C) that can take parafoil airdrop systems from 25,000 feet to accurate landings is a key goal of the Joint Precision Airdrop System. A first instantiation test-flew a 10,000 pound-class parafoil system and has since been extended to accommodate payloads up to 30,000 pounds and as small as a few hundred pounds. The initial avionics applied by the GN&C software used a two-antenna Global Positioning System (GPS) receiver to obtain position, velocity, and heading data. Upgraded avionics now use a single-antenna GPS receiver providing position and velocity combined with inertial sensors providing three-axis acceleration and angular rate data. The guidance algorithm is partitioned into homing, energy management, and an optimized table-lookup terminal flight phase. The control algorithm is a proportional, integral, derivative design with features to deal with system constraints and with feed forward to improve response time. The GN&C software integration and testing is accomplished using a 6 degree-of-freedom simulation with both software-only and hardware-in-the-loop forms. GN&C with the original avionics enabled the 10,000 pound-class parafoil to achieve an expected delivery accuracy of about 150 meters. The GN&C using the new avionics is generalized for on-going tests with payloads ranging from 300 to 30,000 pounds.

Nomenclature

AGL	Above Ground Level
AGU	Airborne Guidance Unit
C	Cost
CARP	Computed Air Release Point
D	Drag
DOF	Degree of Freedom
DZ	Drop Zone
GN&C	Guidance, Navigation, and Control

[1] Principal Member of the Technical Staff, Decision Systems Group, 555 Technology Square/Mail Stop 77.
[2] Senior Member of the Technical Staff, Vehicle and Robotic Systems Group, 555 Technology Square/Mail Stop 23, and AIAA Member Grade.
[3] Laboratory Technical Staff, Mission Design & Analysis Group, 555 Technology Square/Mail Stop 70, and AIAA Fellow.
[4] Principal Member of the Technical Staff, Tactics, Guidance, and Control Group Leader, 555 Technology Square/Mail Stop 77.
[5] Senior Member of the Technical Staff, Cognitive Robotics Group, 555 Technology Square/Mail Stop 77,.
[6] Senior Member of the Technical Staff, Guidance and Control Group, 555 Technology Square/Mail Stop 77, and AIAA Member.
[7] Precision Airdrop GN&C Research Lead, NSRDEC Warfighter Protection and Aerial Delivery Directorate, AMSRD-NSC-WP-AJ/Kansas Street, and AIAA Member.

GPS	Global Positioning System
h	Altitude above MSL
h_G	Ground altitude
$HWIL$	Hardware-in-the-Loop
INS	Inertial Navigation System
J	Controller cost function
$JPADS$	Joint Precision Airdrop System
K	Controller gain
L	List
MP	Mission Planner
MSL	Mean Sea Level
PID	Proportional, Integral, Derivative
RF	Radio Frequency (wireless)
$SODAR$	Sound Detection and Ranging
SW	Software
S	Controller closed-loop sensitivity function
T	Controller closed-loop transfer function
U	Control command
v	Parafoil air speed
w_x	X-component of wind velocity
w_y	Y-component of wind velocity
w_z	Z-component of wind velocity
x	Parafoil along-track position
y	Parafoil cross-track position
γ	Flight path angle
δ	Control actuator deflection angle
ψ	Relative heading
ω	Frequency

I. Introduction

Precision airdrop from high altitude using carrier aircraft that can release payloads from substantial horizontal offset from the desired payload delivery destination is a rapidly developing area of military capability. The implementation of the capability has been motivated both by a need to re-supply soldiers operating in remote areas and to provide means to mitigate urgent humanitarian crises. With a precision airdrop capability in place it is possible to address these needs rapidly, with minimum hostile risk to carrier aircraft that release aerodynamic decelerator systems, and with confidence that the delivered cargo will be received by the intended parties when and where they expect it.

A wide variety of steerable decelerators are being developed to meet the precision airdrop need [Ref. 1]. These systems are fundamentally un-powered, unmanned aerial vehicles requiring an autopilot to provide autonomous, precision flight management after mid-air release. A Guidance, Navigation, and Control (GN&C) subsystem is the enabling component of an autonomous autopilot. To this end, one of the key goals of the Joint Precision Airdrop System (JPADS) program has been the development of an autonomous GN&C subsystem that enables precision delivery of parafoil decelerator systems with a wide range of payload capacities. As the primary customer for the precision airdrop capability, the government benefits in terms of future airdrop capability development cost and schedule from owning an open architecture, autonomous GN&C design that is available for application by steerable decelerator system developers.

The JPADS GN&C subsystem goals include:

- Means for guiding parafoil decelerator systems autonomously from altitudes up to 25,000 above Mean Sea Level to accurate landings at targeted Drop Zone (DZ) locations.
- Algorithm robustness to dispersed decelerator system dynamics response and flight conditions.
- Application of the subsystem to both small and large parafoil decelerators,
- Handling of user-supplied waypoints.
- Government ownership of the resulting open architecture software (SW).
- Efficient and cost-effective integration with the separately developed JPADS Mission Planner (MP).

Government and commercial work on autonomous guided decelerator capabilities began almost 15 years ago. Among the government-sponsored work was joint Draper Laboratory/NASA demonstration of precision parafoil GN&C using a combination of Global Positioning System (GPS) data and an Inertial Navigation System (INS) for the flight path and air-relative state determination [Refs. 2-3]. Resulting flight demonstrations in 1996 showed that this GN&C approach could realize better than 50 m payload delivery accuracy for a small parafoil (88 ft. sq. planform with ~ 170 lb payload). The potential to scale the GN&C design from this system to much larger parafoils was demonstrated only by simulation at the time.

Beginning in 1998, the Army and Air Force began to focus on more effective ways to plan high altitude precision airdrop on-board carrier aircraft. This led to the successful development and demonstration of a laptop computer-based MP to facilitate ballistic and steerable decelerator delivery accuracy when using C-130 and C-17 carrier aircraft [Refs. 4-9]. The initial focus of this program was to assimilate all available atmospheric density and wind data in the vicinity of the DZ and to derive Computed Air Release Points (CARPs) from the carrier aircraft that assured accurate payload deliveries. Subsequently, the MP was extended to derive mission plans for steerable airdrop systems that account for updated atmospheric data and mission objectives, with means provided to wirelessly transmit the plans to the airdrop systems shortly before their release.

Draper Laboratory, one of the developers of the MP, began work on autonomous GN&C SW for the JPADS program in 2004. The initial instantiation of the GN&C SW was used to autonomously fly the Para-Flite 10,000 pound-class *Dragonfly* parafoil airdrop system in an extensive series of flight tests. Those tests were accomplished using an Airborne Guidance Unit (AGU) integrated by Wamore using avionics provided by Robotek [Refs. 10-11]. This GN&C SW has since been extended to accommodate parafoils with payloads up to 30,000 pounds as well as parafoils with payloads as small as a few hundred pounds. The GN&C SW capability extension was conducted in tandem with introduction of an upgraded Wamore AGU using avionics provided by Robot Solutions.

The GN&C SW has been set up to accept wireless mission file data from the MP [Ref. 12]. MP updates to the JPADS GN&C SW can provide new DZ target coordinates, an update of expected winds during descent, as well as details about the airdrop system payload mass and the specific decelerator canopy selection (given that some airdrop system providers may have several canopy sizes that can be applied).

Numerous flight tests were performed using the GN&C SW with the original avionics and the 10,000 pound-class *Dragonfly* system. Flight testing is now in progress with the several hundred pound-class *Microfly* system and the 30,000 pound-class *Megafly* system (all of which use Para-Flite parafoil canopies).

The ensuing sections of this paper will address the following topics:

- The GN&C SW and associated AGU hardware architecture.
- The current design of the GN&C algorithms.
- The GN&C development and verification simulations.
- Some flight test results.
- Future GN&C capability development plans.

II. The GN&C Subsystem Architecture

The initial AGU implementation with which the GN&C SW operated had a two-antenna GPS receiver that provided position, linear velocity, and 1-dimensional heading as the sole navigation data source. The original AGU avionics also had a small, low-cost processor and very limited memory capacity. The upgraded AGU has a single-antenna GPS receiver that provides position and linear velocity data combined with inertial sensors that provide three axis acceleration and angular rate data and a much more capable processor with greatly increased memory capacity.

The current architecture for the avionics system and GN&C algorithms is shown in Figure 1. Changes to accommodate the avionics upgrade are limited to the navigation function. The motivation for the navigation component changes are use of military grade GPS components and cost. The dual-antenna GPS receiver used in the original AGU prototypes was a commercial-off-the-shelf component that was not designed to accommodate military-grade standards. Once a decision was made to go with a GPS receiver that is compliant with military-grade standards for operational systems, cost considerations dictated use of a single-antenna GPS receiver supplemented by low-cost inertial sensors. The upgraded AGU now also has means to accommodate additional experimental sensors. The initial instantiation shown in Figure 1 is a precise, ground-relative altitude sensor provided by Creare that could be used by the GN&C to assure proper timing of pre-landing parafoil flares to minimize ground-relative payload touchdown velocities and improve landing accuracy.

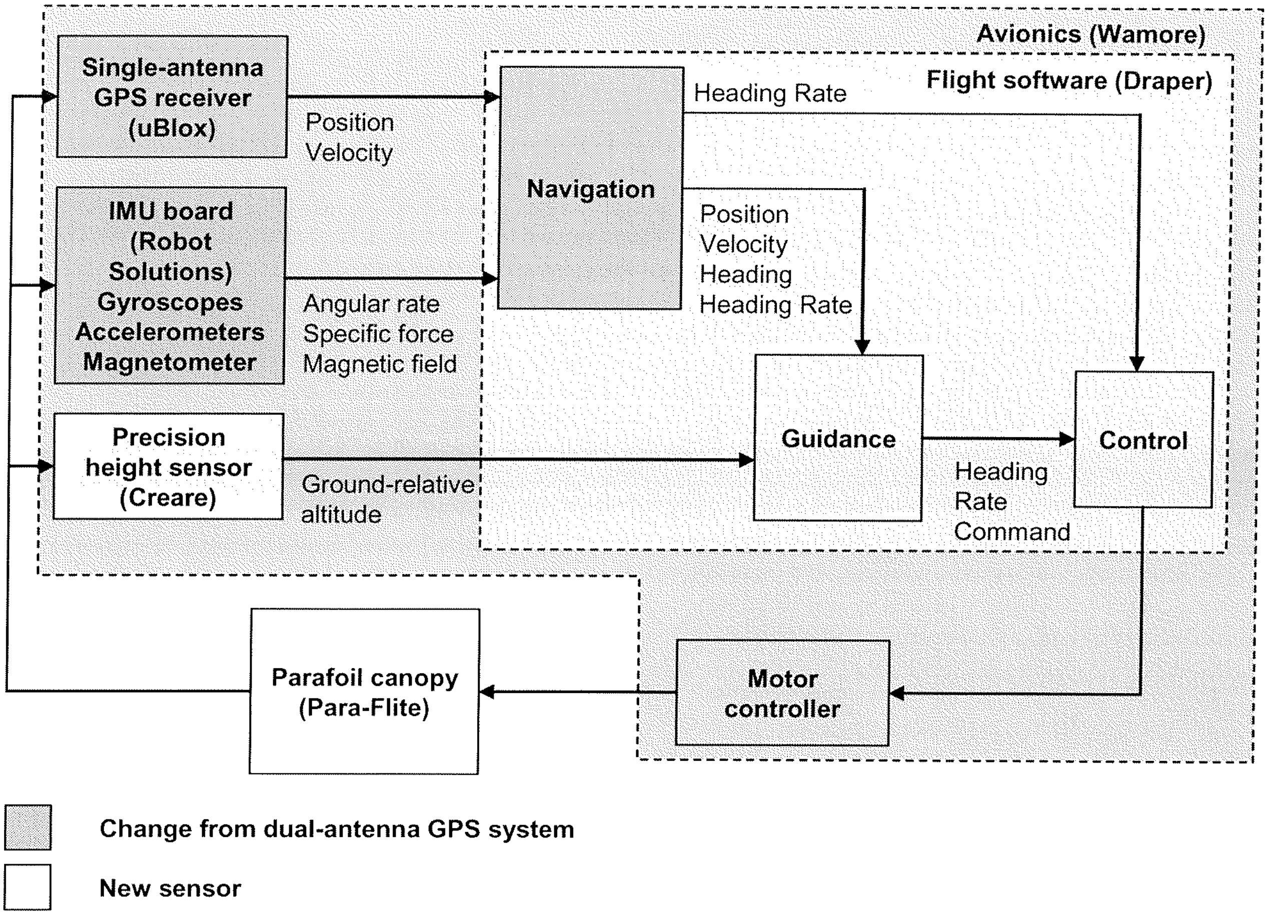

Figure 1: GN&C Block Diagram

III. Current GN&C Algorithm Design

The parafoil GN&C must process the available inertial state data to derive ground and air-relative states, and must use that information to construct and steer the vehicle through a trajectory that reaches the target while dissipating excess energy (in the form of altitude) and passing through any designated way points. Navigation derives the necessary state data. Guidance determines and commands the desired trajectory. Control limits the airdrop system errors in following the path directed by guidance and maintains system stability. Parafoil control achieves the flight path management by relying on deflection of both sides of the canopy trailing edges either differentially (toggling) or together (braking). Depending on the particular parafoil, more or less of the trailing edge is deflected to achieve control. It is a characteristic of parafoils that their glide ratio is insensitive to brake setting, which restricts the guidance and control design envelope. Some of the details of the individual navigation, guidance, and control algorithm features applied in the JPADS application are discussed in the following subsections.

A. Navigation

While GPS-derived data provides direct measurements of the position and velocity of the parafoil, information about the heading angle and wind velocity must also be taken into account in the guidance algorithm. If one such piece of information is known, the other can be derived based on some knowledge of the system model. In particular, if the wind velocity is known, this can be subtracted from the ground-relative velocity provided by GPS to obtain an air-relative velocity, and an assumption of zero sideslip produces a heading estimate. Alternatively, if heading is known, this information can be combined with an assumption of zero sideslip and a model-based estimate of airspeed to obtain air-relative velocity, and also wind velocity when the GPS velocity is subtracted. As a result, the navigation problem reduces to one of determining the heading angle. Additional measurements beyond those that can be obtained from a single-antenna GPS receiver are needed in order to estimate heading.

An integrated GPS/INS navigation solution provides observability into a vehicle's attitude by comparing the change in GPS position and velocity between measurements with the change expected by integrating the outputs of inertial navigation sensors. As long as there is sufficient specific force (any acceleration not due to gravity) acting on the system, any attitude error will manifest itself as a difference between velocity changes observed by a GPS receiver and by inertial sensors, with this difference used to identify actual vehicle attitude. The integrated navigation algorithm used for the JPADS airdrop system application is implemented as a Kalman filter as depicted in Figure 2.

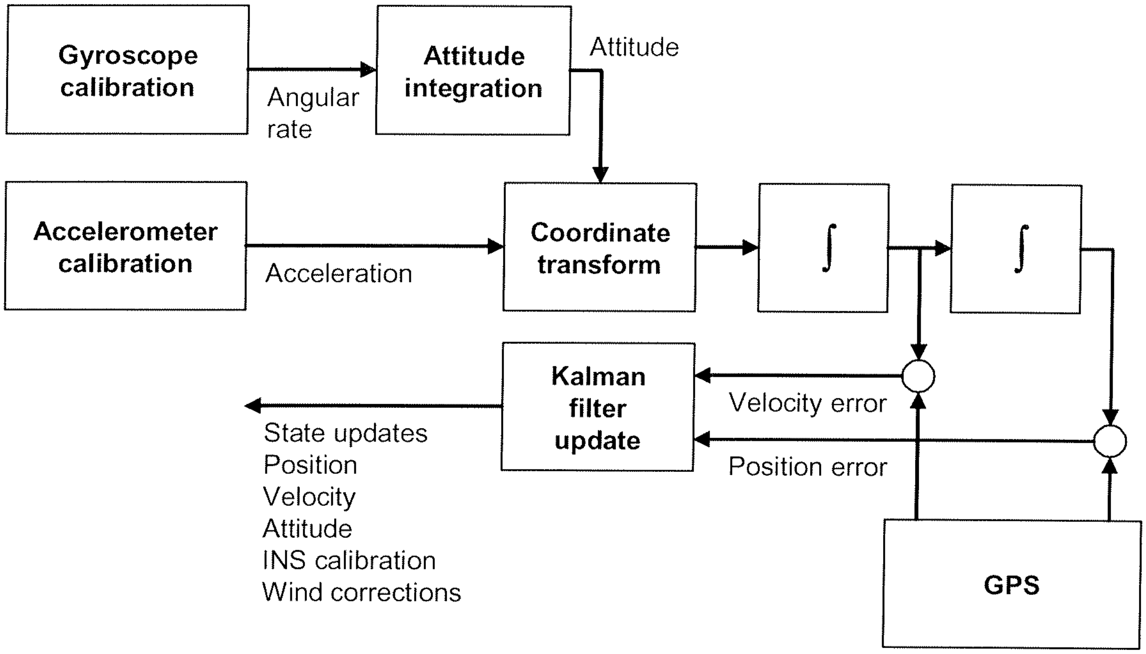

Figure 2: GPS/INS Navigation Architecture

An alternative navigation formulation that uses the GPS measurements and only a single yaw gyro instead of a full six-axis INS was implemented for initial flight tests using the upgraded AGU. This formulation used the yaw gyro in conjunction with a dynamic model of the parafoil to integrate heading and to correct for gyro bias and scale factor errors. An advantage of this approach is that it allows for further cost reduction of the avionics by requiring only a single gyro. However, the additional robustness of the full GPS/INS solution may justify the presence of the additional low-cost inertial sensors in a complete INS.

A challenge that arises in both of these formulations is initialization of the heading angle. In the current GN&C implementation, a winds-aloft forecast is used to initialize the wind velocity estimate vector, and the heading angle is derived from the air-relative velocity vector as described earlier.

Use of a magnetometer (an electronic compass) is also often considered as an inexpensive source of heading data for airdrop system navigation. Use of this sensor type has not to date been part of the GN&C design baseline because of concerns about the unpredictable effects of disturbances to the magnetometer's field measurements resulting from electro-magnetic emissions of other AGU components. However, it is possible that a magnetometer could provide an effective alternative means for initializing the vehicle heading angle.

B. Guidance Overview

Guidance accepts position, velocity, heading, heading rate, and the corrected table of wind velocity vs. altitude from Navigation, and generates heading rate commands which it passes to Control. The guidance strategy is organized by modes which correspond to the four phases of flight. Figure 3 shows the ground track of a simulated flight, colored to show these modes.

Far from the desired impact point, Guidance generates homing commands, i.e., heading rate commands which point the parafoil's velocity toward the target (which is at the origin of Figure 3). Closer to the desired impact point, if the vehicle altitude is still high, Guidance steers to fly a figure-eight pattern; this is called energy management. During the final portion of the descent, guidance steers a trajectory which intersects the desired impact point at a heading which is specified in the mission file. Final heading is generally chosen so that the system lands into the predicted wind, to minimize speed at impact. Near the ground, the control lines are fully retracted to further reduce speed at impact.

The JPADS terminal guidance problem can be stated as follows: Specify commanded heading rate as a function of navigated position, heading, and heading rate so as to reach a prescribed final position, heading, and heading rate. The terminal guidance is now implemented as a table-lookup algorithm, using a large family of pre-computed heading rate commands stored in flash memory. The following subsection shows how dynamic programming was used to generate the table applied to terminal guidance.

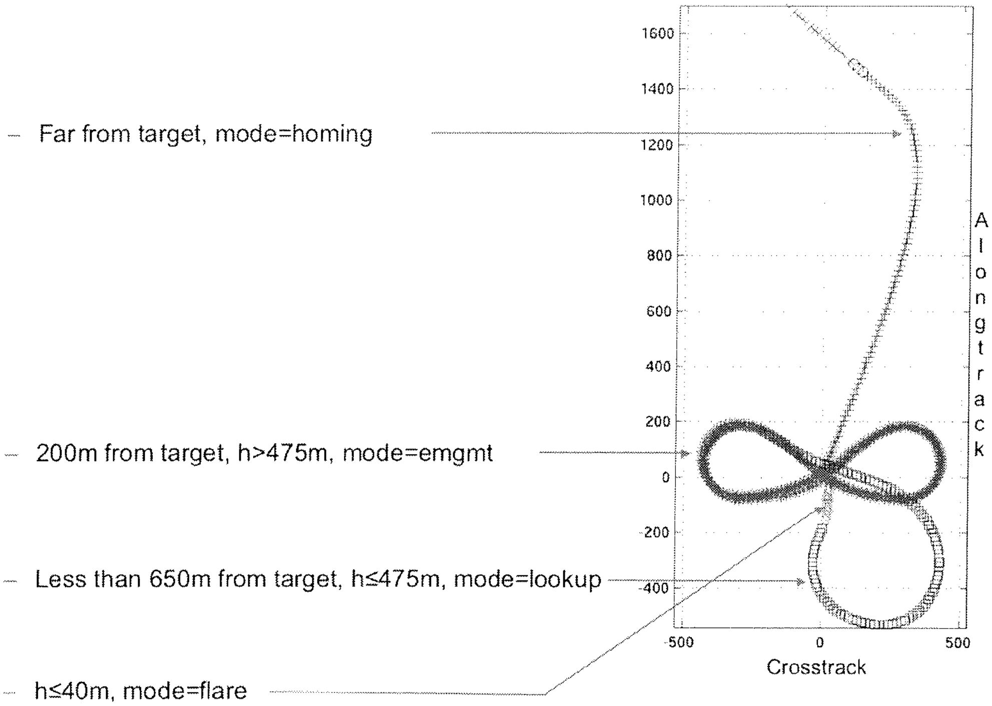

Figure 3: Flight Phases and Guidance Modes

C. Terminal Guidance Solution Using Dynamic Programming

Let x and y denote the along-track and cross-track coordinates of parafoil position in a frame whose origin is at the desired impact point, and let h denote navigated altitude above Mean Sea Level (MSL). The "along-track" direction is the mission-specified landing direction. Let v denote parafoil airspeed. The along-track, cross-track, and down coordinates of velocity with respect to the air mass are $v\cos\gamma\cos\psi$, $v\cos\gamma\sin\psi$, and $v\sin\gamma$, where γ is the flight path angle and ψ is the relative heading (zero in the desired landing direction). Let w_x, w_y, and w_z denote the components of wind velocity. Equation 1 provides the motion model:

$$\begin{aligned} \dot{x} &= v\cos\gamma\cos\psi + w_x \\ \dot{y} &= v\cos\gamma\sin\psi + w_y \\ \dot{h} &= -v\sin\gamma - w_z \\ \ddot{\psi} &= \frac{\dot{\psi}_{cmd} - \dot{\psi}}{\tau} \end{aligned} \tag{1}$$

Note that we assume heading rate exhibits a first order lag response tracking its command. This is a simplification. We make the following additional assumptions:

- Air speed v is a known function of heading rate $\dot{\psi}$ and MSL altitude h
- Flight path angle γ is a known function of $\dot{\psi}$
- The components w_x, w_y, and w_z of wind velocity are known functions of x, y, and h
- MSL altitude of the ground terrain is a known function $h_G(x,y)$ of the position coordinates x and y

The problem is to select a function $\dot{\psi}_{cmd}$ of the five variables x, y, h, ψ, and $\dot{\psi}$. Once this function is specified, the equations of motion determine a unique trajectory from each given initial state $(x_0, y_0, h_0, \psi_0, \dot{\psi}_0)$ to its corresponding terminal state $(x_T, y_T, h_T, \psi_T, \dot{\psi}_T)$ characterized by $h_T = h_G(x_T, y_T)$. We want x_T, y_T, ψ_T, and $\dot{\psi}_T$ to be zero if possible.

To determine the function $\dot{\psi}_{cmd}$, introduce the *minimum miss cost* $C(x,y,h,\psi,\dot{\psi})$. Dynamic programming is the process of evaluating $C(x,y,h,\psi,\dot{\psi})$ recursively for all $(x,y,h,\psi,\dot{\psi})$ in a sufficiently large neighborhood of the target. The cost for our application is provided in Equation 2:

$$C(x,y,h,\psi,\dot{\psi}) = \begin{cases} x^2 + y^2 + \kappa \tan^2 \dfrac{\psi}{2} + \lambda \dot{\psi}^2 & , \quad h \le h_G(x,y) \\ \min_{\dot{\psi}_{cmd}} C(x+dx, y+dy, h-dh, \psi+d\psi, \dot{\psi}+d\dot{\psi}) & , \quad h > h_G(x,y) \end{cases} \tag{2}$$

with

$$\begin{aligned} dx &= (v\cos\gamma\cos\psi + w_x)/(v\sin\gamma + w_z)dh \\ dy &= (v\cos\gamma\sin\psi + w_y)/(v\sin\gamma + w_z)dh \\ d\psi &= \dot{\psi}/(v\sin\gamma + w_z)dh \\ d\dot{\psi} &= (\dot{\psi}_{cmd} - \dot{\psi})/(\tau(v\sin\gamma + w_z))dh \end{aligned} \tag{3}$$

We compute explicit values for $C(x,y,h,\psi,\dot{\psi})$ only for points $(x_i, y_j, h_k, \psi_\ell, \dot{\psi}_m)$ which belong to a pre-selected rectangular lattice. When $h_k > h_G(x_i, y_j)$, $C(x_i, y_j, h_k, \psi_\ell, \dot{\psi}_m)$ is computed using a line search technique, interpolating as needed in a table of previously stored values $C(-,-,h_{k-1},-,-)$. Cost-minimizing commands $\dot{\psi}_{cmd}(x_i, y_j, h_k, \psi_\ell, \dot{\psi}_m)$ are stored in a table as they are obtained during this process. This table of commands, written to flash memory, is used for the parafoil terminal guidance.

Table 1 provides sizing details for the guidance command table as currently implemented. Each command is stored as a single byte. We exploit left-right symmetry to avoid tabulating commands for states whose cross-track position coordinate is negative. Total flash memory required is approximately 124 megabytes; which is well within the capacity of inexpensive flash memory chips that are currently available.

Table 1 – Command Table Sizing

Coordinate	***Range***	***Resolution***	***Gridpoints***
Along-track Position	-800 to +400 m	8 m	151
Cross-track Position	0 to +400 m	8 m	51
Altitude	25 to 500 m	25 m	20
Heading	-180 to +180 deg	5 deg	73
Heading Rate	-15 to +15 deg/s	3 deg/s	11
Total Bytes			123,678,060

We've assumed that MSL altitude of the ground terrain is a known function $h_G(x,y)$ of the horizontal position coordinates. High resolution terrain data is, of course, available, and it's an option to recompute the guidance command table some time in advance of each mission. But this can be avoided when MSL altitude in the vicinity of the desired impact point is approximately constant, as has been the case for all test flights of the JPADS GN&C system so far.

Guidance assumes that wind velocity is, at least approximately, a known function of position. There are several ways to obtain wind information while the carrier aircraft is enroute to the drop location:

- Download forecast of wind data from the Air Force Weather Agency or from another source
- Pilot reports from aircraft
- Measurements obtained from dropsondes released by the carrier aircraft or another (possibly unmanned) aircraft
- Personnel near the desired impact location with means to release instrumented balloons

Each of these methods is practical, and the laptop-based JPADS-MP mission planning SW can assimilate multiple sources of wind information to construct a best estimate. In principle, the guidance table could also be computed on the laptop computer while enroute, making use of best information about winds. However, we avoid this computational chore by subtracting anticipated displacement due to wind from navigated position with respect to the target. This is a standard technique, which is called "working in wind-fixed coordinates" [Refs. 13-14]. The dynamic programming calculation of the guidance table is done only once, with the assumption that wind velocity is everywhere zero.

D. Control

The vehicle controller regulates the vehicle's lateral dynamic states only, closing loops around heading or heading rate depending on the guidance sub-mode. In addition, it provides feed-forward augmentation to increase the effective system bandwidth. It computes the amount of line-deflection necessary to produce the desired heading or heading rate command. The controller architecture has an inner heading rate controller and outer heading angle controller as shown in Figure 4.

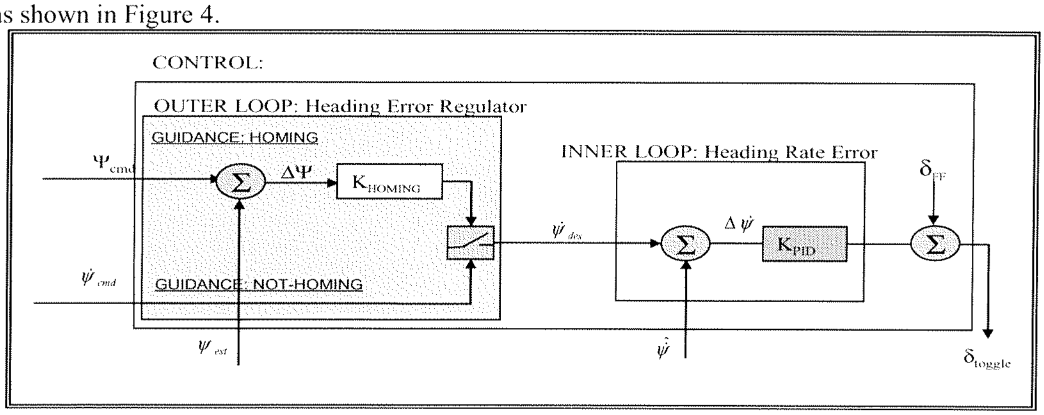

Figure 4: Controller architecture block diagram

1. Heading Rate Controller

The controller inner control loop regulates heading rate error with a straightforward Proportional, Derivative, Integral (PID) implementation given in Equation 4:

$$\delta_{toggle,k} = K_p(\dot\psi_{des,k} - \hat{\dot\psi}_k) + K_I \sum_{j=1\ldots k}(\dot\psi_{des,j} - \hat{\dot\psi}_j) + K_D\left(-\frac{d}{dt}(\hat{\dot\psi}_k)\right) \tag{4}$$

In Guidance homing mode, $\dot\psi_{des}$ is computed from heading error in the outer Control loop, while when Guidance is not in homing mode, $\dot\psi_{des} = \dot\psi_{cmd}$. The integral term includes anti-windup protection and the derivatives are computed using a lateral dynamics estimator. Note that the derivative term is formed from the feedback state signal component only. We choose this structure for the derivative term because guidance commands are most often step commands. Since the derivative of a step command is a delta function, the contribution of the derivative of the heading rate command is mostly zero except when it is very large. Under these conditions the resulting actuator command has a very short duration leading edge spike with each guidance command step which is undesirable for the motors and unnecessary for the vehicle performance since the short spike is too short to induce a response after passing through the plant dynamics. Rather than attempting to smooth or shape the command spike, we choose to ignore it in the heading rate command when taking the derivative.

The PID control gains are derived using optimal control techniques in the frequency domain to best match a weighted combination of a desired transfer function for bandwidth and stability at the lower frequencies and a desired sensitivity function at the higher frequencies for disturbance rejection. The weighted cost function is parametrically defined in Equation 5.

$$J = \min_{Kp,K_I,K_D}\left[\left(\sum_{i=1,\dots N} s_i * (T^{cl\_lp/plant}(\omega_i) - T^{des}(\omega_i))^2\right) + \left(\sum_{j=1:M} r_j * \left((S^{cl\_lp/plant}(\omega_j))^2 - 1\right)\right)\right] \quad (5)$$

Where $T^{cl\_lp/plant}$ represents the closed-loop plant transfer function, T^{des} represents the desired plant transfer function and S^{cl_lp} connotes the closed-loop plant sensitivity function. Note that the last is only analyzed at the higher frequencies where we wish for the system gain to be small and therefore where log(S(ω)) approaches 0. Figure 5 shows the closed-loop transfer function of the tuned controller inner loop based on the plant model identified from flight data for the 30,000 pound-class *Megafly* parafoil.

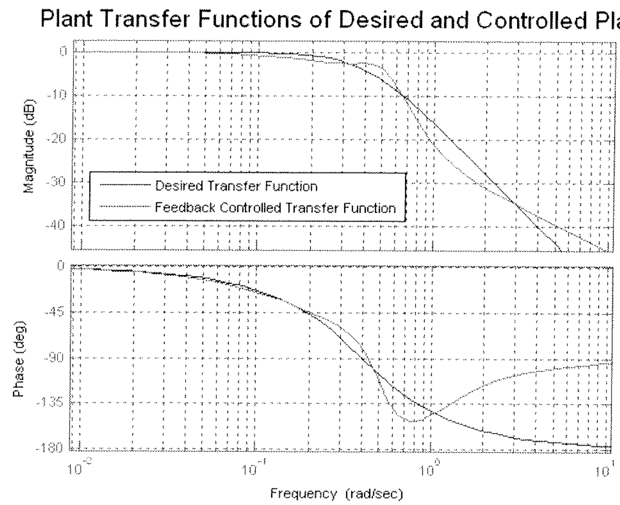

Figure 5: *Megafly* Closed-Loop Plant Transfer Functions

In addition to the feedback form, we augment the heading rate controller with a feed-forward term. The feed-forward signal is computed as follows: (a) given a yaw rate command from guidance, $\dot{\psi}_{cmd}$, invert an idealized steady state plant model to compute the expected steady state control deflection, U_{SS}. (b) Drive a plant model, T^{mdl}, with U_{SS} to compute the expected transient yaw rate at the next time step: $\dot{\psi}_{FF}$ due to the feed-forward term. (c) Drive the feedback controller with this computed $\dot{\psi}_{FF}$. The complete heading-rate controller thus has the form given in Equation 6,

$$\delta_{toggle,k} = K_{FF} \circ \delta_{FF,k} + (1-K_{FF}) \circ \left[K_P \cdot (\dot{\psi}_{FF,k} - \hat{\dot{\psi}}_k) + K_I \cdot \left(\sum_{i=0}^{k} (\dot{\psi}_{FF,i} - \hat{\dot{\psi}}_i)\right) + K_D(-\frac{d}{dt}\hat{\dot{\psi}}_k)\right] \quad (6)$$

where K_{FF} can vary continuously in the set of [0, 1] and reflects how much feed-forward controller input is desired.

2. Heading Controller

The heading controller is an outer control loop that is used when guidance is in its Homing mode when the airdrop system is offset far away from the target. In this mode, it sends desired heading commands to the controller outer loop using Equation 7.

$$\dot{\psi}_{cmd} = K_P^{HOMING} \cdot \Delta\psi + K_D^{HOMING} \cdot (\frac{d}{dt}(\psi_{cmd}) - \hat{\dot{\psi}}) \quad (7)$$

where $\Delta\Psi$ is heading error. Although this controller architecture can be collapsed into a single loop, the multi-loop architecture has the advantage that the heading rate controller is always unchanged and therefore persistent variables such as the integral term, any bias computations and internal variables within the estimator of the derivative of yaw rate never need to be reset.

IV. GN&C Development and Verification Simulations

The GN&C SW integration and testing is accomplished in a configuration-controlled simulation environment. A 6 Degree of Freedom (DOF) simulation exists in both SW-only and Hardware-in-the-Loop (HWIL) forms, with high-fidelity models of applicable parafoils. Both simulation forms and the embedded airdrop system models are addressed in the following subsections.

A. SW-Only Simulation

The SW-only simulation constitutes the formal GN&C algorithm development and verification environment. It was constructed in a modular form that readily enabled its eventual extension to the HWIL (including flight processor-in-the-loop) applications. Developmental and flight versions of the GN&C algorithms are implemented in the SW-only simulation using the flight code form. With high-fidelity airdrop system and environment models included in the SW-only simulation, the facility is used first to run GN&C SW integration tests, then expected GN&C performance tests, and eventually pre-flight GN&C functionality verification tests that address the full GN&C flight envelope.

The SW-only simulation enables Monte Carlo analysis of the integrated GN&C SW performance. This capability is used to determine the expected payload delivery accuracy of the airdrop systems with realistic dispersions statistically applied to the environment and vehicle dynamics models. The Monte Carlo capability also allows evaluation of expected performance changes due to GN&C algorithm modifications such as those applied to accommodate the navigation sensor changes accompanying the AGU upgrade.

The SW simulation is also used for post-flight analysis. Discrepancies in the actual airdrop system flight performance as compared to prediction are addressed by methodologies that seek simulation parameter changes that enable better flight-response representation. The causes of unusual airdrop system stability problems and/or undesired control actuator usage trends, as were observed early in the *Dragonfly* flight test program, also are systematically explored using the simulation, with diagnostic model adjustments made to emulate the observed behavior. The implications of the resulting best-fit model changes are then considered to determine the causes of the undesired behavior and to formulate GN&C-centric mitigation strategies.

The SW simulation currently includes an accurate high fidelity model of the *Dragonfly* parafoil dynamics that factors in many model fidelity improvements based on detailed analysis of data from numerous flight tests. The parameterized simulation models enable application of the simulation to both larger and smaller parafoils. The simulation is now being applied to *Microfly* and *Megafly* GN&C algorithm-related development and test. The fidelity of the *Microfly* and *Megafly* models is being improved as on-going flight test data becomes available.

B. HWIL Simulation

The HWIL version of the Draper JPADS 6-DOF GN&C simulation enables exercise of the parafoil GN&C SW in a real-time environment utilizing most of the flight-specific hardware. In particular, the AGU main processor and subordinate microprocessors are added to the simulation loop to permit a deeper level of flight-code verification. The architecture of this simulation is illustrated in Figure 6. The true flight avionics utilize a number of processors that communicate via an I2C-based synchronous serial bus. In general, this interface was kept intact so that all AGU avionics boards could be utilized unmodified. An added, specialized circuit was created to permit reading of all data passed on this interface.

From the I2C interface data stream, all of the control actuator motor controller commands and feedback are interpreted by the HWIL simulation executive and passed to the dynamics model to tell it the real locations of the control lines based on the actual positions the motor spools achieve. It is important to note that in HWIL simulation implementations to date, no provision is made to provide mechanical loads on the spools. This means that the actuator motors will not react exactly as they would in flight, but the delays in the line motions that they do cause are valuable in the GN&C SW performance evaluation process.

The AGU sensor board supports the accelerometer, gyroscope, magnetometer and GPS sensors. A synthetic-sensor version of this board was developed for the HWIL simulation that permits the simulation processor to send derived sensor values via an asynchronous serial connection which are subsequently converted to analog voltages that are read by the real AGU microcontroller. The GPS receiver is bypassed on this board at the level of the asynchronous serial port that transmits the outputs to the applicable microcontroller.

In addition, the lanyard switch that is pulled in actual flight upon parafoil release from the carrier aircraft is treated in the HWIL simulation as a simple digital output from the simulation processor that manages when the GN&C SW is given an indication that the emulated airdrop system has been "released".

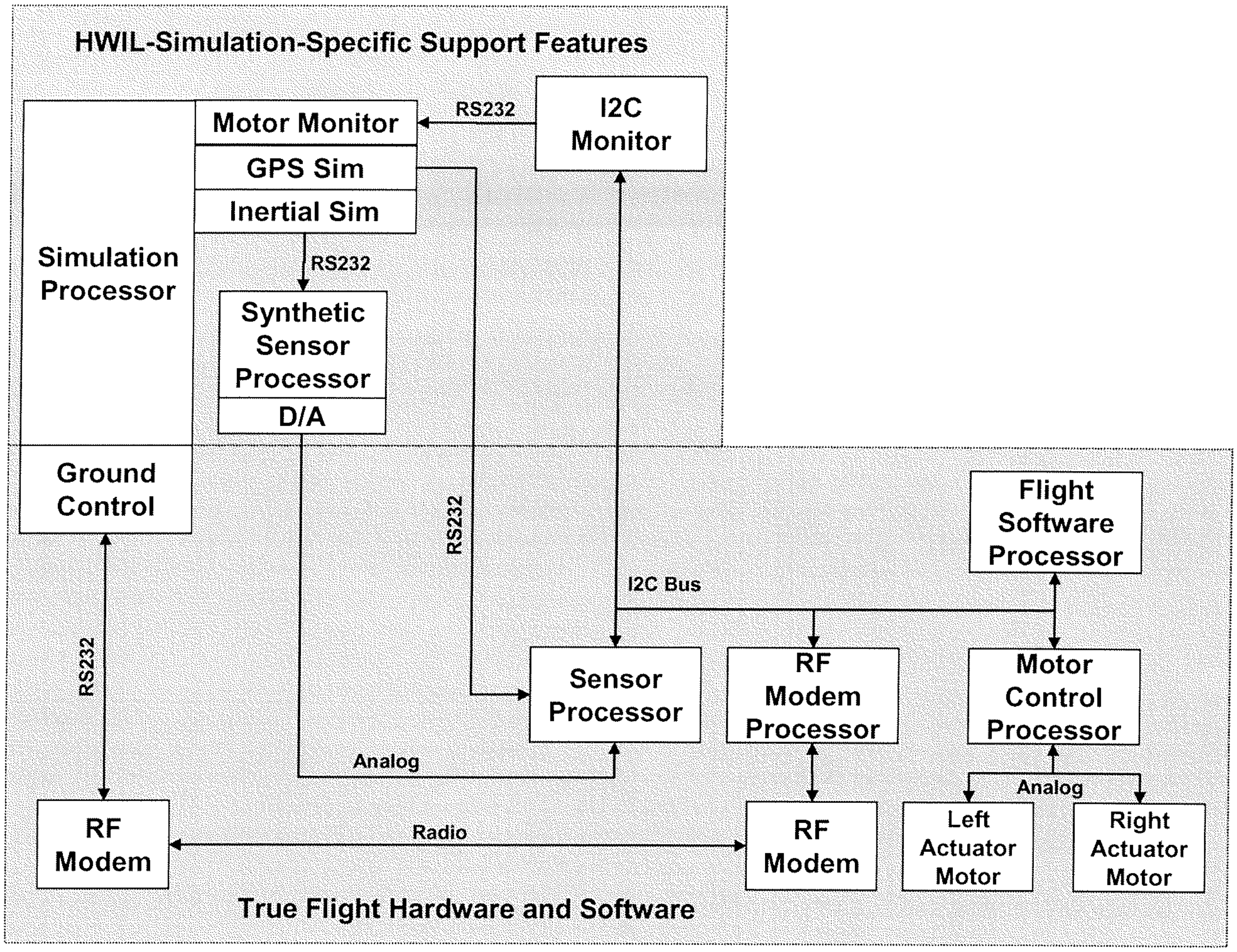

Figure 6: The HWIL Simulation Architecture

C. The Simulated Airdrop System Models

The Draper parafoil simulation models are based on treating the parafoil as a rigid 6-DOF body, complete with apparent mass/inertia derived from theoretical treatments, and aerodynamics derived from flight data. Analysis of static aerodynamic behavior has focused on matching steady-state velocity, glide-slope, and turn rate behavior of the parafoil systems. In particular, a simplified longitudinal Lift-to-Drag ratio (L/D) and flight speed mathematical model was implemented originally for the *Dragonfly* 10K pound-class parafoil system and is subsequently being used as the simulation framework for the 30K pound-class *Megafly* parafoil system and the 300 pound-class *Microfly* parafoil system that is being used as a subscale platform for evaluating the *Megafly* AGU avionics suite. Figure 7 shows the most recent comparison between lift-to-drag and airspeed data taken from a single test flight of the *Megafly* system and a preliminary aerodynamic model (plotted versus the toggle brake setting normalized by a stall toggle of 300 inches) – the comparison is good and the general trend observed with brake toggle is quite similar to extensive data collected on the *Dragonfly* system. More data is needed to fully characterize the *Megafly* longitudinal trim, however initial results indicate the system is capable of an L/D of ~3.5 with an airspeed near 20 m/s (at the flight test weight of 20,000 lbs.).

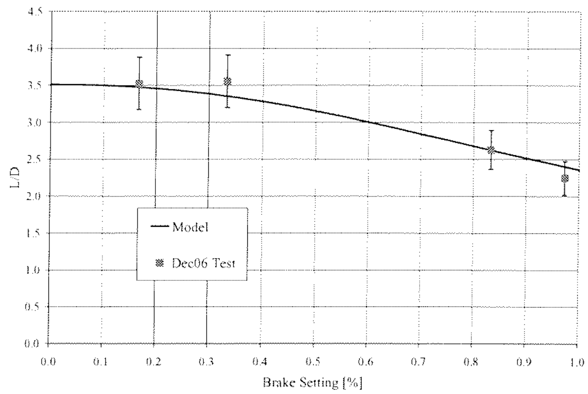

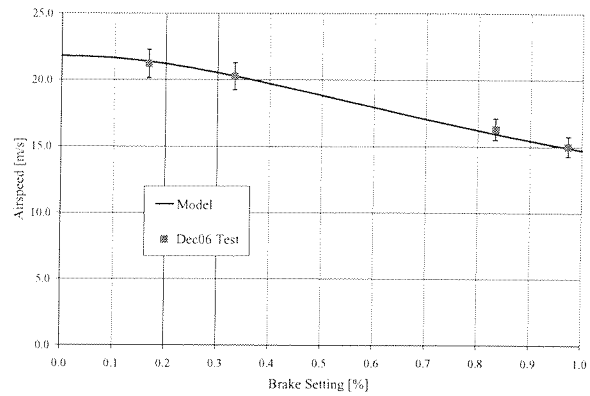

Figure 7: Longitudinal Trim for Megafly

A model for the steady-state turn rate of the *Megafly* system is currently being developed. Early results show that the system is capable of ~5 deg/s of turn rate at a differential toggle of 100 inches, but exhibits significant non-linear behavior at lower toggle brake settings (where the realizable steady-state turn rate decreases substantially). This type of behavior was observed during the X-38 program and will need to be addressed either in the control algorithm or by limiting the minimum toggle setting used during autonomous flights. The parafoil simulation uses a tabular mapping from toggle setting to control yaw torque, and therefore can be adjusted to match any relationship found in flight tests. In addition to steady-state turn rate matching, effort has also been given to matching the transient turn rate behavior of the *Megafly* system. The procedure that has been adopted is to generate manual step differential toggle commands during flight tests, in order to capture both the steady-state and transient turn rate behavior of the system. System identification of previous test flights has shown that a parafoil's heading rate behavior is governed principally by a 2nd order oscillatory "Dutch roll" lateral mode. In the case of *Megafly* this mode has a time constant between 11-12 seconds and a damping ratio of ~0.5 (very well damped). The *Megafly* simulation will be tuned to properly reflect the actual transient behavior by using parameter changes to the model's damping derivatives. In general, more data is required to estimate a complete turn dynamics model for the *Megafly* system, however initial flight test data shows the system exhibits behavior similar in nature to the *Dragonfly* and therefore can be analyzed using the same tool set.

V. Some Flight Test Results

Flight testing and incremental improvement of the GN&C algorithm features with the original avionics enabled the 10,000 pound-class *Dragonfly* system to achieve a Circular Error Probable payload delivery accuracy of about 150 meters. A generalized version of the GN&C SW using the new AGU avionics for payloads up to 30,000 pounds and for much smaller payloads is now undergoing initial flight test evaluation. In the initial stages of development, a surrogate small (man-sized) parafoil system, the *Microfly*, was used to evaluate the upgraded GN&C algorithms and AGU hardware outlined in Section III. Figure 8 shows a trajectory ground-track from a recent flight test of the *Microfly* parafoil system equipped with the upgraded AGU, implementing the GPS + inertial navigation algorithm, and a 5-state guidance look-up table. Figure 8 (complete flight and zoomed final approach) should be compared to Figure 3 detailing the ideal flight guidance modes. The system performs the homing, energy management, look-up, and flare guidance modes coming to rest approximately 75 meters from the target [0,0]. It is evident from the wind-relative trajectory that the system did not perform an accurate estimate of the wind direction, thus causing the asymmetric appearance of the energy management turns. Despite this issue, the system was capable of correcting its final approach with only a small overshoot of the target. Figure 9 shows the turn rate comparison between actual and commanded heading rate for the same flight, along with the actual differential toggle used by the system. It is evident from the plot that the system exhibited excellent heading rate tracking, even during the last stage of the flight.

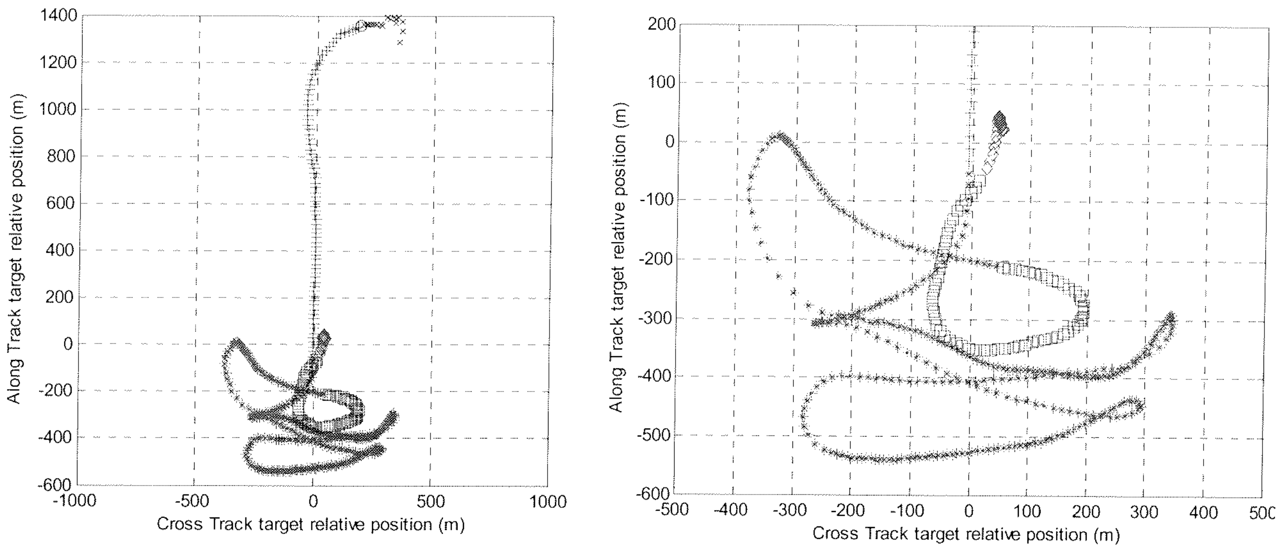

Figure 8: Normalized Ground-track in De-weighted Wind Frame (normal/zoomed)

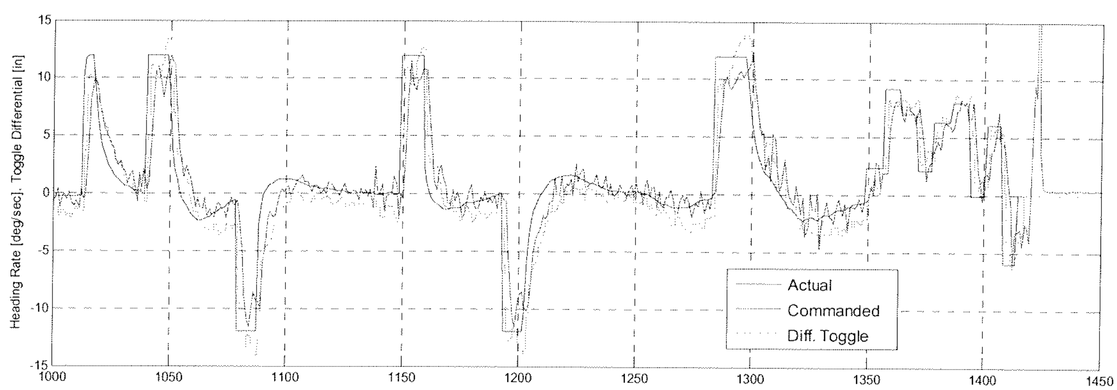

Figure 9: Turn Rate Comparison

VI. Future GN&C Capability Development Plans

The GN&C SW being developed by Draper under the JPADS program will continue to have capabilities added to accommodate an expanding set of airdrop system applications and to enable paylaod delivery accuracy improvements. Several following specific added capability development activities are already in work.

A. Utilization of a Ground-Relative Height Sensor

Creare has developed a Sound Detection and Ranging (SODAR) sensor to make precision determination of the ground-relative altitude of vehicles during terminal descent flight phases. The Draper JPADS GN&C SW is being extended to enable use of the SODAR for accurate detection of the ground-relative position relative to the descending airdrop system over a wide variety of surface types (grass, dirt, water, foliage, etc.). To limit the cost of the unit, the current SODAR sensor is designed with a range selected specifically to support the needs of parafoil decelerators which are under control all the way to the ground. It is designed to provide an accuracy of ±2 feet below 500 feet Above Ground Level (AGL). In particularly benign acoustic conditions, it has detected the surface to about 1000 feet AGL. .The Creare sensor package also outputs data from an auxiliary baro-altimeter to provide descent rate information. By May 2007 the Draper GN&C SW will begin using the SODAR ground-relative height measurement to enable precise timing of parafoil terminal flare maneuvers. Longer term, the SODAR data will be applied to enable proper timing of more complex maneuvers that help to further minimize the touchdown velocity of parafoil airdrop systems. Both the barometric and SODAR measurements will eventually be integrated into the

GPS/INS navigation filter to optimize navigation knowledge relative to the desired impact point on the ground, thereby enabling improved payload landing accuracy.

B. In-Flight Lidar Wind Sensing

The Army is funding research into the design of a miniature, low-cost lidar-based remote wind sensor capable of providing real-time wind speed and direction ahead of an airdrop system while in flight. Some developmental technical challenges remain to be addressed, but when this sensor is available, it will provide an additional data source regarding the ambient environment to the GN&C system. GN&C would use the data to make in-flight refinements to the wind table applied by Guidance to predict the airdrop system trajectory from the start of the terminal flare maneuver to the ground. This would allow Guidance to aim for the point in the sky that is the optimal flare initiation point. Furthermore, the data would help Guidance and Control to reduce the revised flare initiation point errors by application of the in-flight wind data to the airdrop system's trajectory management prior to the flare initiation.

C. Additional Landing Accuracy Improvement Features

New GN&C concepts are being explored that would improve landing accuracy by enabling better management of the terminal vehicle track. Given the added inertial navigation orientation and angular rate data in all vehicle body axes resulting from the new AGU sensors, extensions to the Control system inner loop could be developed that would include explicit feedback-management of the vehicle bank angle and angular rates to enable precision-control of the pre-landing maneuvers, thereby reducing down-track and cross-track landing errors. Effective implementation of this GN&C feature will require development of more precise models than are now available of the expected parafoil airdrop system rotation coupling dynamics during turns. A longer term GN&C capability extension would apply modified parafoil control actuation features that would enable ground-relative glide slope management via airspeed control to further reduce airdrop system down-track errors at landing.

VII. Conclusions

Draper Laboratory has developed GN&C SW for autonomous descent trajectory management of JPADS parafoil airdrop systems. This GN&C SW is modular and parameterized to make it easily extensible to a wide variety of airdrop systems, with on-going work to improve its performance and extend its capabilities. The Navigation algorithm has successfully transitioned from use of a commercial, two-antenna GPS receiver to a militarized single-antenna GPS receiver combined with low-cost inertial angular rate sensors. The Guidance algorithm has a variety of modes as a function of distance and altitude above the target, including an optimized, table look-up scheme for managing the terminal turn into the landing target. The Control algorithm has a heading-rate-driven inner loop, with a heading-driven outer loop that is added when Guidance is in its homing mode while still well away from the target. The Control implementation is PID-based with added features to handle constraints and feed-forward logic to improve response time. A modular 6-DOF SW-only simulation, with high fidelity models of parafoil dynamics supports the development and integration of the GN&C SW. The SW-only simulation is also used in a Monte Carlo mode to evaluate expected GN&C performance and to analyze flight test results. The simulation-based flight test analysis in turn derives updates to the simulation's parafoil models to improve the tool's fidelity. An HWIL extension of the simulation enables verification of the GN&C SW while operating in real-time on actual flight processors, and while interacting with actual flight data buses and control line actuation motors. Flight testing of the GN&C SW with the initial Navigation instantiation (using the two-antenna GPS receiver) that was performed using the 10,000 pound-class *Dragonfly* parafoil airdrop system achieved better than 150 m expected landing accuracy. The GN&C SW has recently been extended for application to parafoils ranging from 300 pound-class payload capability to 30,000 pound-class systems, and is undergoing initial flight tests with airdrop systems at both ends of the payload capacity spectrum. Both additional Navigation sensor additions and new GN&C SW features are being explored to enable on-going improvement in the payload delivery accuracy for airdrop systems in all weight classes that use the Draper-developed GN&C SW.

Acknowledgments

The authors gratefully acknowledge the funding support of Joint Forces Command JPADS Advanced Concept Technology Demonstration, the Office of the Secretary of Defense, the US Army 30K Army Technology Objective, US Army Program Manager Force Sustainment Systems, as well as the US Air Force Air Mobility and Transportation Commands. We would also like to thank the large team of professional system testers at the US

Army Yuma Proving Ground as well as Jim Blumenthal and his team at Kingman, Arizona who helped bring the JPADS – Mission Planner system to the point of initial field use.

The material in this paper is based upon work supported by the US Army Natick Soldier Research, Development and Engineering Center under contract Nos. W9124R-04-C-0154, -0144, -0118, and W9124R-06-C-0110. Any opinions, findings and conclusions or recommendations expressed in this material are those of the authors and do not necessarily reflect the views of the Natick Soldier Research, Development and Engineering Center.

References

[1]Steve Tavan, , " Status and Context of High Altitude Precision Aerial Delivery Systems," presented at the AIAA Guidance, Navigation, and Control Conference, CP-2006-6793, Keystone, Colorado, August 21-24, 2006.

[2]Philip D. Hattis and Richard Benney, "Demonstration of Precision Guided Ram-Air Parafoil Airdrop Using GPS/INS Navigation," presented at the Institute of Navigation's Fifty-Second Annual Meeting, Cambridge, Massachusetts, June 18-20, 1996.

[3]Hattis, P., Appleby, B., Fill, T., and Benney, R., "Precision Guided Airdrop System Flight Test Results," CP 97-1468 presented at the 14th AIAA Aerodynamic Decelerator Systems Conference, CP-97-1468, San Francisco, California, June 3-5, 1997.

[4]Hattis, P., Fill, T., Rubenstein, D., Wright, R., and Benney, R., "An Advanced On-Board Airdrop Planner to Facilitate Precision Payload Delivery," presented at the AIAA Guidance, Navigation, and Control Conference, CP-2000-4307, Denver, Colorado, August 14-17, 2000.

[5]Hattis, P., Fill, T., Rubenstein, D., Wright, R., Benney, R., and LeMoine, D., "Status of an On-Board PC-Based Airdrop Planner Demonstration," presented at the AIAA Aerodynamic Decelerator Systems Conference, CP-2001-2066, Boston Massachusetts, May 22-24, 2001.

[6]Hattis, P., Angermueller, K., Fill, T., Wright, R., Benney, R., and LeMoine, D., "An In-Flight Precision Airdrop Planning System," presented at the 23rd Army Science Conference, Orlando, Florida, December 2-5, 2002.

[7]Hattis, P., Angermueller, K., Fill, T., Wright, R., Benney, R., LeMoine, D., and King, D., "In-Flight Precision Airdrop Planner Follow-On Development Program," presented at the AIAA Aerodynamic Decelerator Systems Conference, CP-2003-2141, Monterey, California, May 19-22, 2003.

[8]Campbell, D, Fill, T., Hattis, P., and Tavan, S.., "An On-Board Mission Planning System to Facilitate Precision Airdrop," presented at the Infotech@Aerospace Conference, CP-2005-7071, Arlington, Virginia, September 26-29, 2005.

[9]Wright, R., Benney, R., and McHugh, J., "On-Board Atmospheric Modeling System to Support Precision Airdrop," presented at the Infotech@Aerospace Conference, CP-2005-7070, Arlington, Virginia, September 26-29, 2005.

[10]Carter, D, George, S., Hattis, P., Singh, L., and Tavan, S., "Autonomous Guidance, Navigation, and Control of Large Parafoils," presented at the AIAA Aerodynamic Decelerator Systems Conference, CP-2005-1643, Munich, Germany, May 23-26, 2005.

[11]George, S., Carter, D., Hattis, P., Singh, L., Berland, J.C., Dunker, S. Markle, B., Lewis, J., Tavan, S., and Barber, J., "The Dragonfly 4,500 kg Class Guided Airdrop System," presented at the Infotech@Aerospace Conference, CP-2005-7095,Arlington, Virginia, September 26-29, 2005.

[12]Hattis, P., Campbell, D., Carter, D., McConley, M., and Tavan, S., "Providing Means for Precision Airdrop Delivery from High Altitude," presented at the AIAA Guidance, Navigation, and Control Conference, CP-2006-6790, Keystone, Colorado, August 21-24, 2006.

[13]Soppa, U., Strauch, H., Goerig, L., and Belmont, J., "GNC Concept for Automated Landing of a Large Parafoil," presented at the AIAA Aerodynamic Decelerator Systems Technology Conference, CP-1997-1464, San Francisco, CA, June 3-5, 1997.

[14]Kaminer, I., and Yakimenko, O., "Development of Control algorithm for the Autonomous Gliding Delivery System", presented at the AIAA Aerodynamic Decelerator Systems Conference, CP-2003-2116, Monterey, California, May 19-22, 2003.